Experimental study of a high-power CW side-pumped Nd:YAG laser

D.L. Yu*, D.Y. Tang

School of Electrical and Electronic Engineering, Nanyang Technological University, Singapore 639798, Singapore

Abstract

The paper reports on the characterization of a side-pumped 40 W CW Nd:YAG laser. A side-pumping configuration with six laser diodes is used for the laser. We show the comparison between the calculated and measured pump energy distributions in the laser crystal. The birefringence and the thermal lens effect of the Nd:YAG crystal have been experimentally investigated, and their influence on the performance of the laser are discussed. Output power and beam quality of the laser under different output couplings, cavity lengths, types of cavity and different temperatures of the cooling water have been experimentally studied.
© 2002 Elsevier Science Ltd. All rights reserved.

Keywords: Nd:YAG laser; Thermal lensing; Birefringence; Optical resonator

1. Introduction

Although there have been several different pump configurations of high-power laser diodes (LDs) pumped Nd:YAG lasers developed recently, the side-pumped Nd:YAG rod laser is still a kind of compact and simple design with high electrical-to-optical efficiency [1–7]. In order to improve the pumping efficiency and the beam quality of a diode-side-pumped Nd:YAG rod laser, several techniques in delivering pumping beams have been proposed; generally an uniform pumping power distribution within the rod gain medium is preferred to cancel the bifocusing of the thermal lens [8–12]. As the thermal lens and the birefringence caused by the temperature gradients across the laser rod play a crucial role in determining the output power and beam quality of a laser, apart from their analytical description, a thorough experimental investigation of the effects on a practical laser system such as the one reported in the paper, in particular, also to relate their effects to the laser performance, e.g. the experimental input–output relation, laser efficiency, laser beam quality under different cavity parameters and conditions could be useful. We have set up such an experimental system to conduct these researches.

In this paper, we will first briefly describe our compact and simple 40 W CW Nd:YAG laser system, especially its diode-side-pumping configuration. We will then present our studies on the birefringence, thermal lensing and pump energy distribution of the laser system under non-lasing condition. The output power and beam quality of the laser under different cavity parameters, cooling water temperature and an adjustable aperture inside the cavity will also be presented in the paper.

2. Side-pumping configuration of the laser

In order to pump the full cross section of the laser rod and to achieve a high spatial overlap between the pump radiation and the resonator mode, a side-pumping configuration as shown in Fig. 1 is designed for our 40 W CW diode pumped solid-state laser. The pump module comprises of six 40 W CW operating LDs side pumping the laser crystal. The six LDs are divided into two groups, which are spatially displaced along the crystal axis. Each group consists of three LDs. Within one group the three LDs are distributed symmetrically around the crystal. The angular positions of the LDs between the two groups have a rotation of $41°$. The laser beam from each diode laser is coupled onto the laser rod by a cylindrical lens. A quartz tube of $\phi = 10$ mm is used to seal the cooling water of the crystal.

The pump energy distribution inside the laser crystal has been simulated, from which the temperature distribution in the cross section of the laser crystal could also be estimated. Experimentally, the pump distributions were measured by observing the fluorescence intensity profile using an AGEMA Infrared Systems under the condition that there

---

* Corresponding author. Tel.: +65-6790-5456; fax: +65-6790-4161.
E-mail address: edlyu@ntu.edu.sg (D.L. Yu).
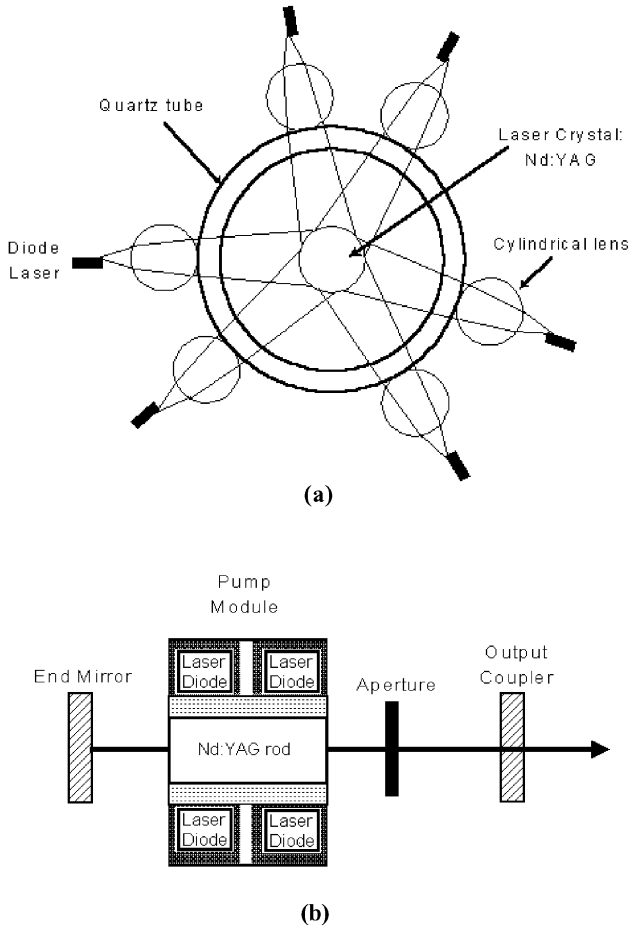
(a)

(b)

Fig. 1. Pumping configuration (a) and schematic of the laser cavity configuration (b) of the engineering model DPSS laser.

was no lasing of the laser. Fig. 2 shows the measured and calculated pump distributions in the laser rod with the six LDs pumping configuration. The experimental results show a good agreement with the calculated ones.

3. Study of the thermally induced effects

3.1. Birefringence

After the pump distribution had been calculated and measured experimentally, we further investigated the strength of the thermally induced birefringence in the laser. Our next aim was to know quantitatively how strong is the effect induced in our laser under the current pumping configuration, as the appearance of the effect could cause significant decrease in the laser output power and the beam quality. An experimental set up as shown in Fig. 3 was used to study the thermally induced birefringence of the laser crystal. The laser beam from a commercial He–Ne laser was first expanded and then collimated to illuminate the laser crystal. A polarizer was used to polarize the He–Ne laser beam before

it is incident on the laser crystal. A polarization analyzer was used to analyze the polarization change of the He–Ne beam after it passes through the laser crystal.

Without pumping, the polarizer and the analyzer will be so adjusted that no light can pass through the analyzer. When the laser crystal is pumped, because of the appearance of the thermally induced birefringence, the probe light suffers from depolarization when passing through it, and consequently, will be partially transmitted through the analyzer. The transmitted light forms the so-called isogyres, which display the geometrical loci of constant phase difference. Photographs of the transverse intensity patterns of the He–Ne laser beam under various pump powers of our laser are shown in Fig. 4. The temperature of the cooling water in the laser system was fixed as 16°C.

Only one ring can be seen in Fig. 4 indicating that the phase retardation of the He–Ne laser beam is not more than one wavelength, suggesting that the thermally induced birefringence in our laser is not served. This experimental result indicated indirectly that the pump beam distribution in our laser is quite uniform.

3.2. Thermal lens effect

The focal length of thermal lens effect depends on both temperature gradients and stresses in the laser rod. In order to quantitatively measure the thermal lens effect of this laser, we have designed an experiment similar to that shown in Fig. 3 to measure the focal length of the thermal lens. The experimental procedure used to measure the thermal lens is as follows: we first expand and collimate the He–Ne laser beam, and then let it pass through the laser crystal while the laser is pumped by the LDs. We identify the smallest beam waist of the He–Ne laser beam and then measure the distance of the beam waist to the center of the laser crystal. When the pump power strength is changed, the variations of the He–Ne laser beam in the beam diameter could be clearly seen on a screen. The measured thermal focal length and its variation with increase in pumping power under different temperatures of the cooling water are plotted in Fig. 5.

The results of the measurement show that the thermal focal length decreases with the increase of the pumping power. The lower the temperature of the cooling water is, the shorter is the initial focal length. However, under high pumping power, the focal length seems not so sensitive to the temperature of the cooling water and the focal length does not vary exactly as the inverse of pumping power.

4. Studies on laser performance

Fig. 6 shows a comparison of the output powers of the laser under different output coupling with a fixed cavity length of 165 mm. One end mirror of the laser cavity is a concave mirror of radius of curvature of 900 mm and reflectivity $R = 100\%$.
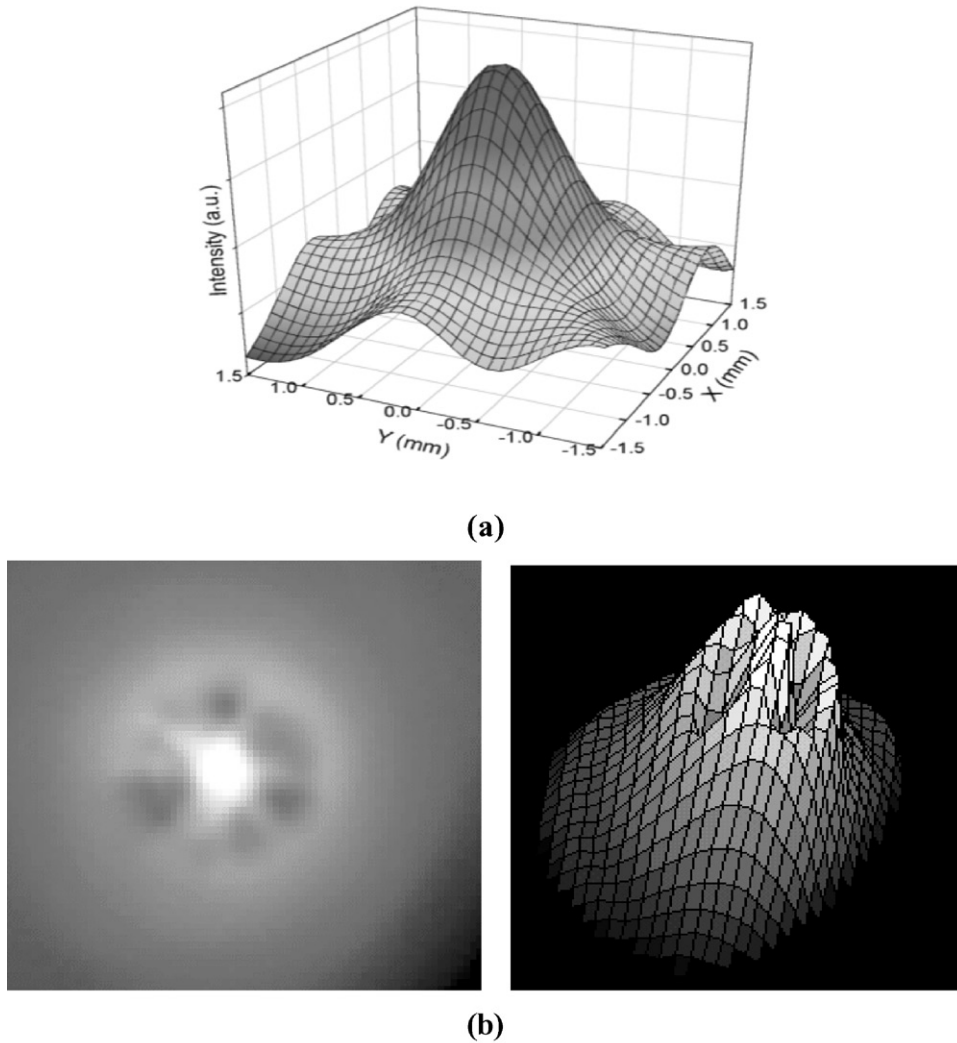
(a)

(b)

Fig. 2. Calculated (a) and measured (b) pump energy distributions for a six-side-pumping Nd:YAG rod.
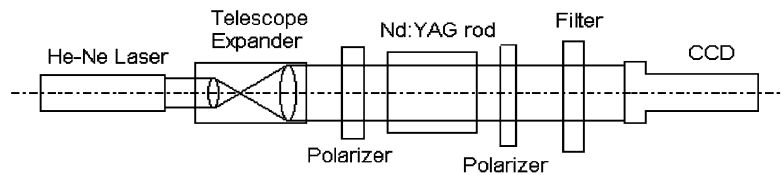

Fig. 3. Schematic of the birefringence effects.

The maximum output power was obtained with an output mirror of 6% output coupling. Higher or lower output coupling degrades the output performance of the laser.

In order to further study the variation of output power with the types of laser cavity, we had also investigated the performance of the laser with different kinds of the cavity mirrors. A result is shown in Fig. 7.

It is to be noted that the plano/concave resonator has the highest output power under the current cavity length. Considering the existence of a thermal lens in the cavity, it could be understood why this cavity configuration could give even higher output than the plano/plano one. Obviously, the cavity configuration has the largest active gain volume.

Figs. 8(a) and (b) show a comparison of the output powers of the laser with different cavity lengths. Fig. 8(a) shows the cavity with 10% output coupling and Fig. 8(b) that with 6% output coupling.

In all our experiments, we found that a cavity length of 165 mm gave the best laser output power.
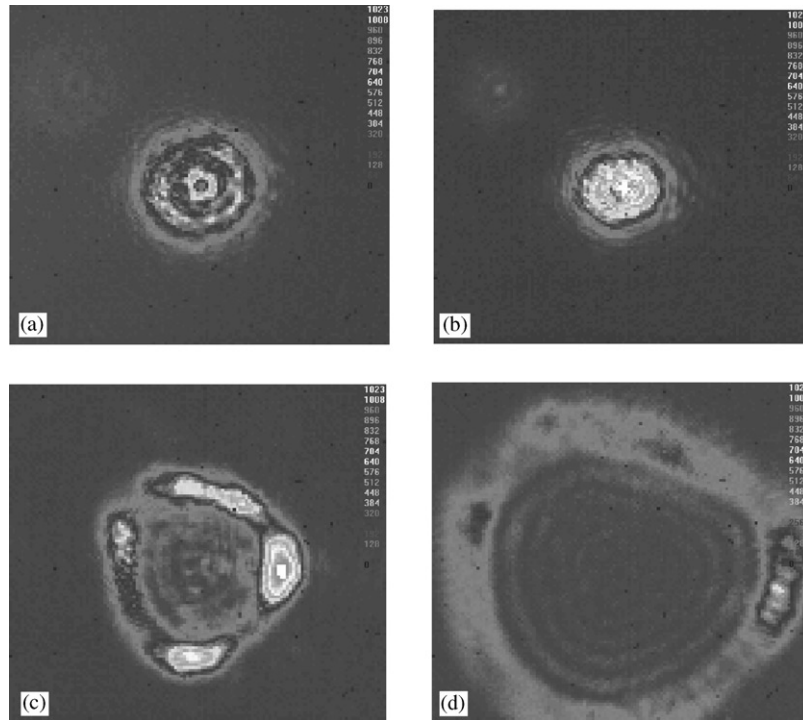
Fig. 4. Effect of the thermally induced birefringence in the laser; from (a) to (d) the pump power is increased: (a) 0 W, (b) 90 W, (c) 180 W, and (d) 240 W.
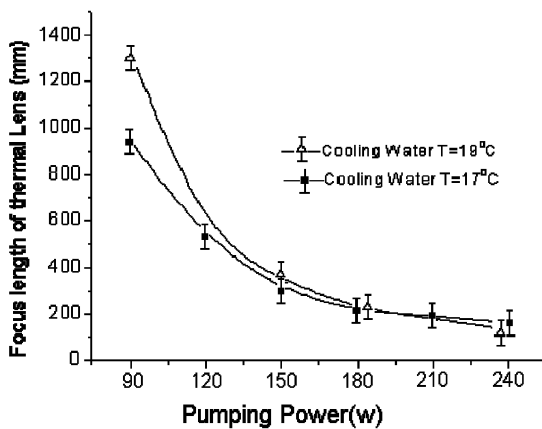

Fig. 5. Thermal focal length at different pumping powers.

Fig. 6. Output power at different pumping powers.

The flow of cooling water takes away the heat generated in the laser rod and on the LD holders. The temperature of the cooling water will not only affect the value of temperature of the thermal equilibrium in the system, but also all the thermal effects induced in the system, such as the strength of the focal lens, thermally induced birefringence, etc., which in turn affect the output power and the quality of the laser beam of the laser. Fig. 9 shows the output power of the laser under operation of different temperatures of the cooling water.

The other parameters of the cavity are given in the figure. It is to be noted that the laser has the maximum output
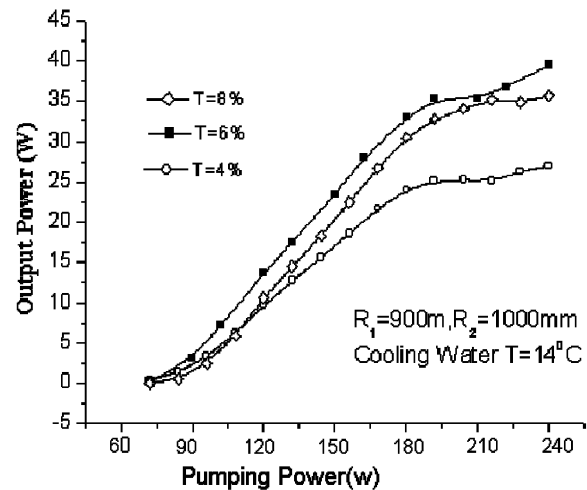
power when the cooling water temperature is about 11.0°C. We also found from the experiments that the value of oscillation threshold on driving current varies as the inverse of the cooling water temperature, showing the effect of the temperature dependence of the LD emission wavelength. In another experiment, we have separately cooled the LDs and laser crystal with water of different temperatures, and found that the optimum temperature of the water for cooling the laser crystal is about 17°C.
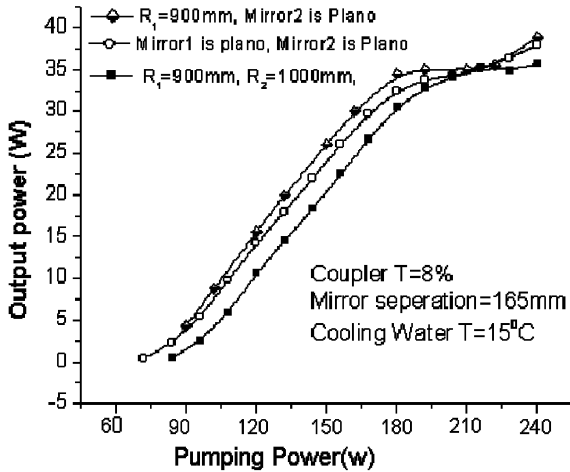
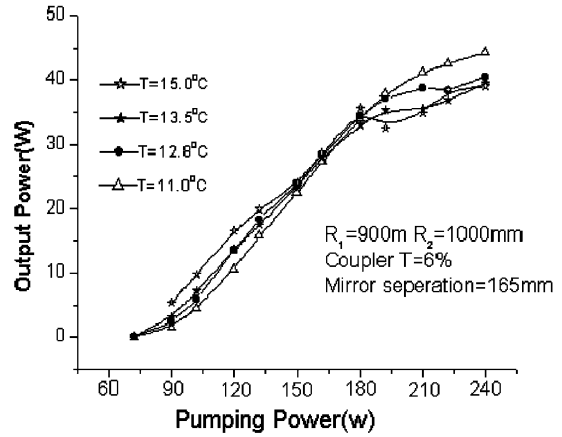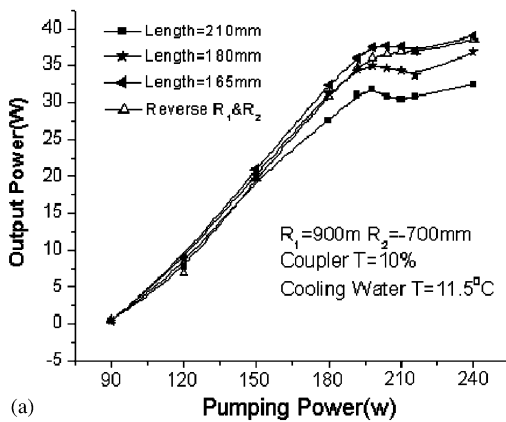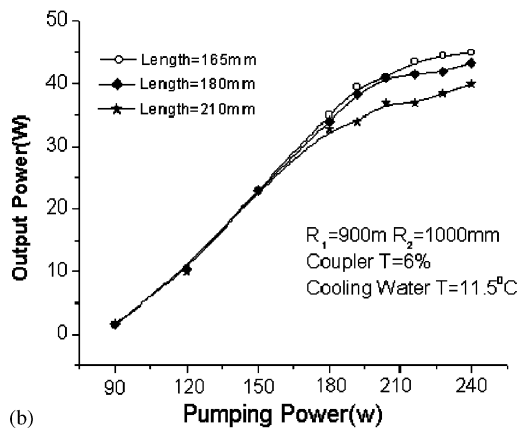Fig. 7. Output power under different types of cavity.

Fig. 9. Output power under operation of different temperatures of the cooling water.

(a)

Fig. 10. Value of M^2 vs. different LDs pumping power.

(b)

Fig. 8. Output power of the laser with different cavity lengths: (a) $T = 10\%$ and (b) $T = 6\%$.

Fig. 10 shows the output beam M^2 value of this laser under different pump strengths.

From Fig. 10, we could conclude that the quality of the output laser beam degrades with the increase of the pumping power. In our experiments, we found that the pure fundamental mode (TEM_{00}) operation of the laser can only be obtained when the output power is not larger than 1 W.
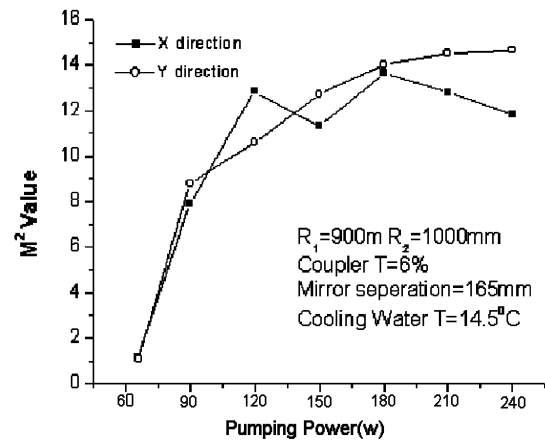
Otherwise multi-transverse mode operation of the laser was observed. In order to operate the laser at the fundamental mode and prevent the appearance of the higher-order transverse modes, an adjustable aperture is inserted in the laser resonator. As the higher-order modes have a larger spatial extent than the fundamental mode, they will experience larger loss than the fundamental mode; hence they could be suppressed. Even though the existence of an aperture in the resonator could prevent the appearance of the high-order transverse modes, the thermally induced effects, such as the birefringence and a thermal lens always exist, so with strong pump the laser system could still not output the laser beam of ideal fundamental mode. Fig. 11 gives the laser profiles under different incident pump powers even with a suitable aperture in the resonator. When the incident pumping power is 90 W (LD driving current is 15 A), the output power of the laser system is 0.1 W. When the pumping power is 240 W (LD driving current is 40 A) we obtained a maximum output power of 9.5 W. The output power is about one-fourth of the value of the laser when no aperture was inserted to the cavity.
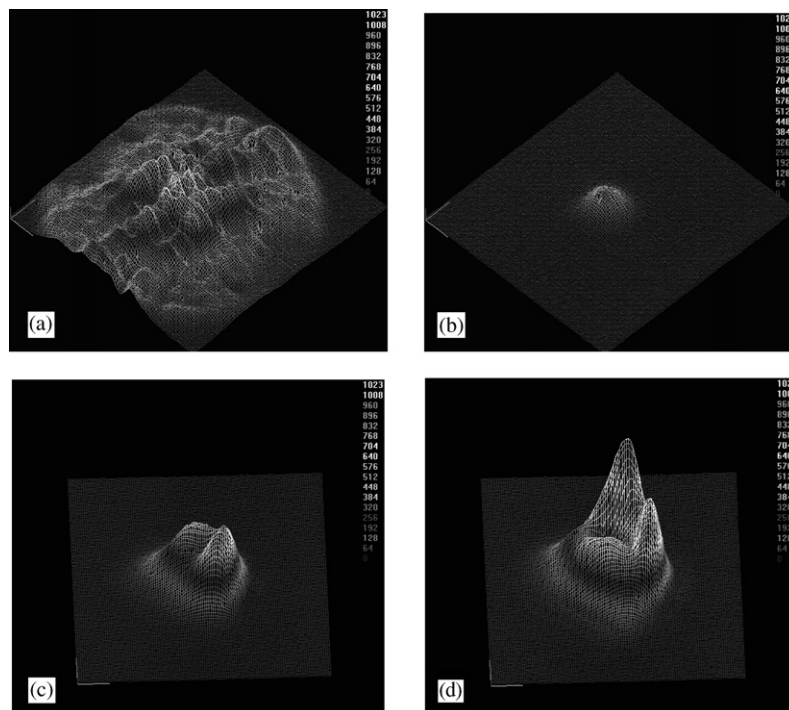
Fig. 11. Output beam profile and output power vs. pumping power with an aperture: (a) No aperture 240–40 W (b) 90–0.1 W (c) 180–5.4 W (d) 240–9.5 W.

5. Conclusion

From the above characterization and results of the laser system, we found that the current pump configuration could provide a good pump beam uniformity in the laser cavity, and result in less birefringence effect in the laser crystal. An optimized operation condition for the laser output power and the laser beam quality was also experimentally determined, namely the cavity length should be about 165 mm, the output coupling about 6%, and the temperature of the cooling water about 11.0°C. The possibility of using an intra-cavity aperture to control the laser beam quality has been experimentally tested. These experimental results could be useful as a guideline for the design of compact, high-power LD-side-pumped Nd:YAG lasers.

References

[1] Shuichi Fujikawa, Keisuke Furuta, Koji Yasui. 28% electrical-efficiency operation of a diode-side-pumped Nd:YAG rod laser. Opt Lett 2001;26(9):602–4.

[2] Shuichi Fujikawa, Tetsuo Kojima, Koji Yasui. High-power and high-efficiency operation of a CW-diode-side-pumped Nd:YAG rod laser. IEEE J Sel Top Quantum Electron 1997;3(1):40–4.

[3] St Pierre RJ, Mordaunt DW, Injeyan H, Berg JG, Hilyard RC, Weber ME, Wickham MG, Harpole GM, Senn R. Diode array pumped kilowatt laser. IEEE J Sel Top Quantum Electron 1997;3(1):53–8.

[4] Hugel H. New solid-state lasers and their application potentials. Opt Lasers Eng 2000;34:213–29.

[5] Shepherd DP, Hettrick SJ, Li C, Mackenzie JI, Beach RJ, Mitchell SC, Meissner HE. High-power planar dielectric waveguide lasers. J Phys D 2001;34:2420–32.

[6] Rutherford TS, Tulloch WM, Sinha S, Byer RL. Yb:YAG and Nd:YAG edge-pumped slab lasers. Opt Lett 2001;26(13):986–8.

[7] Baker HJ, Chesworth AA, Pelaez Millas D, Hall DR. A planar waveguide Nd:YAG laser with a hybrid waveguide-unstable resonator. Opt Commun 2001;191:125–31.

[8] Masaki Tsunekane, Shuetsu Kudo, Katsujj Mukailhara, Hideyuki Moribe, Takashi Ooyama. Diode-laser side-pumped solid-state laser device. US Patent Application Publication. Publication No. US2001/oo33596A1.

[9] Koechner W. Solid-state laser engineering, 5th ed. Berlin: Springer, 1999.

[10] Schmid M, Weber R, Graft T, Roos M, Weber HP. Numerical simulation and analytical description of thermally induced birefringence in laser rods. IEEE J Quantum Electron 2000;36(5): 620–6.

[11] Honea EC, Ebbers CA, Beach RJ, Speth JA, Skidmore JA, Enanual MA, Payne SA. Analysis of an intracavity-doubled diode-pumped Q-switched Nd:YAG laser producing more than 100 W of power at 0.532 μm. Opt Lett 1998;23(15):1203–5.

[12] Susumu Konno, Shuichi Fujikawa, Koji Yasui. 206 W continuous-wave TEM_{00} mode 1064 nm beam generation by a laser-diode-pumped Nd:YAG rod laser amplifier. Appl Phys Lett 2001;19(17):2696–7.